

DEL: Dense Event Localization for Multi-modal Audio-Visual Understanding

Mona Ahmadian
University of Surrey
m.ahmadian@surrey.ac.uk

Amir Shirian
JPMorgan Chase
amirdonte15@gmail.com

Frank Guerin
University of Surrey
f.guerin@surrey.ac.uk

Andrew Gilbert
University of Surrey
a.gilbert@surrey.ac.uk

Abstract

Real-world videos often contain overlapping events and complex temporal dependencies, making multimodal interaction modeling particularly challenging. We introduce **DEL**, a framework for dense semantic action localization, aiming to accurately detect and classify multiple actions at fine-grained temporal resolutions in long untrimmed videos. DEL consists of two key modules: the alignment of audio and visual features that leverage masked self-attention to enhance intra-mode consistency and a multimodal interaction refinement module that models cross-modal dependencies across multiple scales, enabling high-level semantics and fine-grained details. Our method achieves state-of-the-art performance on multiple real-world Temporal Action Localization (TAL) datasets, UnAV-100, THUMOS14, ActivityNet 1.3, and EPIC-Kitchens-100, surpassing previous approaches with notable average mAP gains of +3.3%, +2.6%, +1.2%, +1.7% (verb), and +1.4% (noun), respectively. The source code will be made publicly available.

1. Introduction

Temporal action localization (TAL) is a crucial and challenging task in video understanding, focusing on identifying the temporal boundaries of action instances and classifying them within untrimmed videos [41]. Understanding real-world scenes and events is inherently a multimodal perception process, integrating visual and auditory cues to achieve comprehensive video understanding [18, 30, 32]. For instance, distinguishing between a person speaking and merely mouthing words is difficult with visual information alone, as both actions involve similar lip movements. Incorporating audio cues, however, helps resolve this ambiguity by detecting the presence or absence of vocal sounds. Despite the complementary nature of visual and audio information, modeling multimodal interactions remains chal-

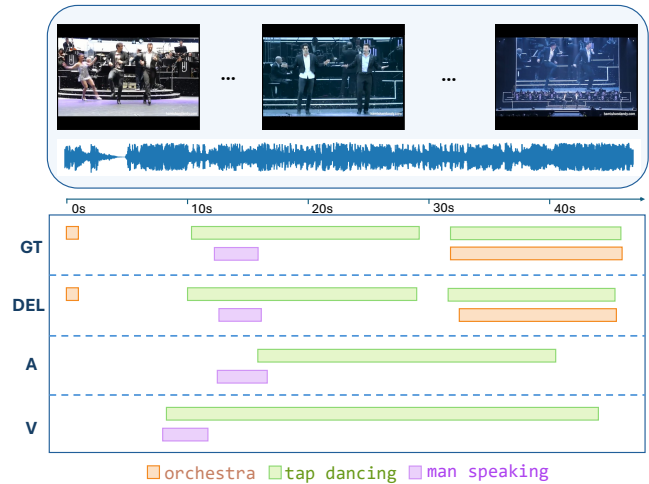


Figure 1. Real-world videos contain overlapping events of varying durations, making precise localization challenging. The image presents ground-truth (GT) annotations alongside the predictions of DEL, an audio-only model (A), and a visual-only model (V). The unimodal models struggle with a certain category. In contrast, **DEL** effectively detects and classifies both short and long-duration events, even when they co-occur, demonstrating its superior multimodal fusion capability.

lenging due to modality misalignment, the length of the actions, and the complex interplay of cross-modal dependencies—particularly in videos with overlapping, concurrent events [40].

Prior efforts have made progress in Audio-Visual Event Localization (AVE) for trimmed videos, where each video typically contains a single, isolated audio-visual event [12, 33, 42]. Unlike AVE, dense localization of audio-visual events requires identifying and recognizing all events within an untrimmed video, capturing short and long-duration interactions that may overlap [3, 9, 13, 17]. Recent advances have demonstrated the effectiveness of transformer net-

works and Feature Pyramid Networks (FPN) for TAL [37, 46, 53, 58], significantly improving performance by leveraging multi-resolution visual features. However, those approaches overlook the role of audio.

A persistent challenge in audio-visual event localization is the effective extraction and fusion of information across modalities, especially when multiple events co-occur. Traditional approaches either process audio and visual streams independently or rely on late fusion, limiting their ability to model fine-grained temporal dependencies. Moreover, most multi-modal methods employ pretrained models to extract features, which, while beneficial for representation learning, often lead to misaligned features due to differences in pretraining objectives and domain shifts between audio and visual modalities. Additionally, contrastive learning techniques often focus on instance-level alignment while neglecting intra-video relationships such as temporal coherence and cross-event correlations, crucial for distinguishing similar events occurring at different times.

To address this challenge, we propose **DEL**, a novel framework designed to model cross-modal dependencies while explicitly preserving fine-grained temporal structure. Our approach enables precise temporal alignment and fine-grained spatial understanding across multiple audio-visual events. DEL uses a multi-scale fusion strategy, ensuring robust event localization even in densely overlapping scenarios. We incorporate two key modules into our transformer-based model: 1) a **multimodal adaptive attention mechanism** using a masked self-attention mechanism that ensures temporal coherence and intra-modal consistency within the audio-visual information. 2) a **path aggregation network** that introduces multiple temporal resolutions to capture fine-grained and high-level semantics in the sequences.

Additionally, we introduce an intra-sample contrastive loss to refine feature discrimination within a single data mode and an inter-sample contrastive loss for better alignment of audio-visual representations across different samples. Instead of manually defining positive and negative samples, our method introduces a feature scoring mechanism that enables the model to automatically assign confidence scores and select contrastive pairs during training. This enhances feature discrimination and cross-modal coherence for precise event localization. We demonstrate state-of-the-art performance on multiple benchmarks, including UnAV-100 [13], THUMOS14 [17], ActivityNet 1.3 [3], and EPIC-Kitchens-100 [9], achieving significant improvements over prior methods.

2. Related Works

2.1. Single-Modality Temporal Localization Tasks

Deep learning has significantly advanced temporal action localization (TAL), enabling the detection and classification

of actions in untrimmed videos. TAL methods are generally categorized into two-stage and single-stage approaches. Two-stage methods generate action proposals with confidence scores before refining and classifying them [22, 23]. In contrast, single-stage approaches directly localize actions in a single pass, eliminating the need for proposal generation. Our work follows a single-stage TAL.

These methods can be further classified into anchor-based [6, 28, 44, 59] and anchor-free approaches [21, 29, 48, 49, 54]. Anchor-based methods employ predefined multi-scale temporal anchors to detect potential action segments, refining their boundaries through regression techniques. Conversely, anchor-free methods predict action boundaries directly by modeling temporal dependencies or regressing distances to action start and end points.

Recent advances integrate graph neural networks (GNNs) [51, 54, 57] and transformers [5, 39, 43] to enhance temporal modeling. Transformers, in particular, have demonstrated superior performance by leveraging self-attention mechanisms to capture long-range dependencies. Inspired by progress in object detection [8, 35] and saliency detection [21], recent state-of-the-art approaches incorporate transformer-based feature pyramid networks (FPNs) [7, 37, 46, 58]. These networks effectively combine multi-scale feature representation with classification and regression heads, improving accuracy and efficiency over conventional methods.

2.2. Multimodal Audio-Visual Event Localization

While joint audio-visual representation learning has been extensively studied in video retrieval and classification [1, 19, 50], its application in TAL is less explored, primarily due to the challenges of modality misalignment and the need for fine-grained temporal modeling. Most existing methods assume that the audio and visual events are perfectly aligned [2, 40, 55], limiting their effectiveness in real-world settings where events may be asynchronous or overlapping. As highlighted in our introduction, real-world scenarios often involve a complex interplay between modalities and concurrent events.

Current audio-visual TAL models employ two-stage late fusion strategies, where audio and visual modalities interact only at the final classification stage. This approach reduces their ability to model fine-grained temporal dependencies, making them less effective for complex event localization. Some recent approaches incorporate cross-attention mechanisms [25, 34, 47, 52] but operate at fixed temporal scales and lack dynamic fusion control.

Furthermore, contrastive learning techniques [16, 45] often focus on instance-level alignment while neglecting intra-video relationships, such as temporal coherence and cross-event correlations, which are crucial for distinguishing similar events occurring at different times. This limita-

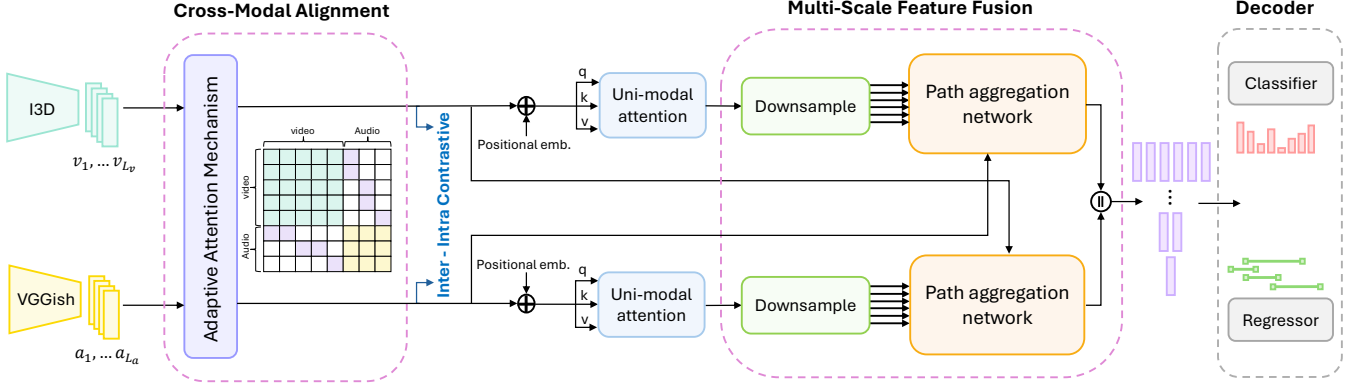


Figure 2. Overview of our proposed **DEL** framework. Our model integrates (1) an *adaptive attention mechanism* for aligning audio and visual features, (2) *inter- and intra-sample contrastive learning* to enhance event discrimination, and (3) a *multi-scale path aggregation network* for feature fusion. \parallel represents the concatenation operation.

tion affects their ability to handle multi-scale variations and modality-specific characteristics. Our DEL framework explicitly models cross-modal dependencies to address these challenges while preserving fine-grained temporal structure through an adaptive attention mechanism and a path aggregation network. Moreover, our dual contrastive learning strategy, incorporating inter-sample and intra-sample contrastive loss, refines feature discrimination within a single video, addressing the limitations of existing methods.

3. Method Overview

Fig. 2 provides an overview of our framework. Given the untrimmed audio-visual input, the dense action localization task aims to precisely detect the temporal boundaries of action instances, requiring the refinement of their semantic representations. To begin with, we tokenize the audio and visual data using existing feature extraction networks. Our method then aligns and fuses audio-visual features for precise event localization through three key modules: (1) We employ an adaptive attention mechanism for cross-modal alignment, which dynamically aligns the audio and visual representations. (2) Next, score-based contrastive learning helps to dynamically select inter and intra mode hard-negative samples to improve feature discrimination in the training process. (3) Finally, our path aggregation network for multi-scale feature fusion facilitates multi-scale feature extraction by generating multiple temporal representations and aggregating them to enhance temporal modeling.

3.1. TAL Problem Formulation

We formulate dense audio-visual event localization as a joint event classification and boundary estimation problem. Given a video with audio-visual data, we segment it into T paired segments, represented as

$$\mathbb{S} = \{(\mathbf{V}_t, \mathbf{A}_t)\}_{t=1}^T, \quad (1)$$

where \mathbf{V}_t and \mathbf{A}_t denote the visual and audio features at time t . Note that the number of segments, T , varies across videos. The ground-truth annotation is defined as

$$\mathcal{G} = \{g_n = (\tau_{start,n}, \tau_{end,n}, \lambda_n)\}_{n=1}^N, \quad (2)$$

where $\tau_{start,n}$ and $\tau_{end,n}$ indicate the event boundaries and $\lambda_n \in \Lambda$ represents the event class from a defined set of $|\Lambda|$ categories and N is the total number of events in the video.

During inference, our model predicts localized events

$$\hat{\mathbb{S}} = \{\hat{s}_t = (\delta_{start,t}, \delta_{end,t}, q(y_t))\}_{t=1}^T \quad (3)$$

where, $q(y_t) \in [0, 1]^{|\Lambda|}$ is the event classification probability, and $\delta_{start,t}$ and $\delta_{end,t}$ represent estimated temporal offsets of the current time t for event boundaries. The final predictions are:

$$\begin{aligned} \hat{\lambda}_t &= \arg \max_{\lambda \in \Lambda} q(\lambda_t), \\ \hat{\tau}_{start,t} &= t - \delta_{start,t}, \\ \hat{\tau}_{end,t} &= t + \delta_{end,t}. \end{aligned} \quad (4)$$

This results in the fine-grained localization and classification of overlapping audio-visual events.

3.2. Adaptive Attention for Cross-Modal Alignment

To address misalignment between audio and visual data in the videos, we propose an adaptive attention mechanism that dynamically adjusts feature importance, ensuring effective synchronization of corresponding audio and visual signals and enhancing cross-modal coherence. To compute this adaptive attention, an attention mask \mathbf{M} , is initialized with the sizing, $\mathbf{M} \in \mathbb{R}^{(L_v+L_a) \times (L_v+L_a)}$, where L_v and L_a denote the lengths of the video and audio features from the sequences, respectively. Then, given a concatenated input $\mathbf{X} = [\mathbf{V}|\mathbf{A}] \in \mathbb{R}^{(L_v+L_a) \times d}$ where \mathbf{X} contains both video

and audio features, we construct the query (\mathbf{Q}) and key (\mathbf{K}) matrices via linear transformations:

$$\mathbf{Q} = \mathbf{X}\mathbf{W}_Q, \quad \mathbf{K} = \mathbf{X}\mathbf{W}_K, \quad \mathbf{V} = \mathbf{X}\mathbf{W}_V \quad (5)$$

where $\mathbf{W}_Q, \mathbf{W}_K, \mathbf{W}_V \in \mathbb{R}^{d \times d}$ are learnable projection matrices. Next, we compute the adaptive attention as:

$$\text{aat}_{i,j} = \frac{m_{i,j} \exp(\mathbf{Q}_i \mathbf{K}_j^T / \sqrt{d})}{\sum_k m_{i,k} \exp(\mathbf{Q}_i \mathbf{K}_k^T / \sqrt{d})} \quad (6)$$

where $i, j \in [1, L_v + L_a]$ represent the indices of the adaptive attention matrix, \mathbf{AAT} . The mask \mathbf{M} aims to emphasize and learn feature interactions corresponding to the same event across both intra and inter modality. For intra-modality, we apply a standard global attention mechanism, allowing features within the same modality to attend to each other by setting the corresponding entries in the mask to 1. For cross-modality, only entries corresponding to the same temporal segment are assigned a value of 1, ensuring focused interactions between aligned video and audio features. The attention mask is then applied to the adaptive attention matrix from the self-attention mechanism, guiding modality-specific and cross-modal feature interactions.

3.3. Score-based Contrastive Learning

We adopt a score-based contrastive learning objective to improve the relationships between the audio-visual features within a video at training time. Unlike standard contrastive learning methods, which rely on predefined sampling heuristics, our method dynamically selects contrastive pairs using a learned score function that ranks the audio-visual features based on contextual similarity and temporal alignment. We use both inter-sample and intra-sample objectives. The inter-sample strengthens relationships between similar input video and audio pairs in a batch, while intra-sample learning captures fine-grained temporal relationships within the same sample in a single data modality.

Inter-Sample Contrastive Learning. Given a batch of sample pairs, we employ an inter-sample contrastive loss that maximizes the cosine similarity between the $[CLS_V]$ and $[CLS_A]$ tokens of matched video-audio pairs while minimizing the similarity between tokens from mismatched pairs. The $[CLS_V]$ and $[CLS_A]$ tokens are global representations of the video and audio features, respectively. They are extracted from the adaptive attention layer of their respective modality and designed to capture high-level semantic information. The inter-sample contrastive loss is defined as:

$$\begin{aligned} \mathcal{L}_{\text{inter}} = & \mathbb{E}_{z \sim [CLS_V]_j, z^+ \sim [CLS_A]_j, z^- \sim I_{k \neq j} [CLS_A]_k} \ell(z, z^+, z^-) \\ & + \mathbb{E}_{z \sim [CLS_A]_j, z^+ \sim [CLS_V]_j, z^- \sim I_{k \neq j} [CLS_V]_k} \ell(z, z^+, z^-) \end{aligned} \quad (7)$$

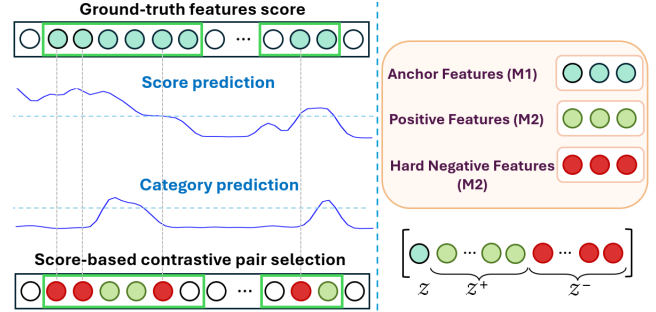


Figure 3. Score-based contrastive pair selection for identifying positive and hard-negative samples for each anchor within the event segment of a single modality. M1 represents the modality chosen as the anchor, while the goal is to select corresponding positive and hard-negative features from another modality represented as M2. Token-level predictions (score s_t and category c_t) provide early supervision that refines latent features. This early processing guides the contrastive selection of hard-negative samples.

where $\ell(z, z^+, z^-)$ represents the standard contrastive loss [14], defined by the following equation, and τ is a learnable temperature parameter.

$$\ell(z, z^+, z^-) = -\log \left(\frac{\exp(z^T \cdot z^+ / \tau)}{\exp(z^T \cdot z^+ / \tau) + k \exp(z^T \cdot z^- / \tau)} \right) \quad (8)$$

Intra-Sample Contrastive Learning with Score-Based Pair Selection.

As shown in Fig. 3, unlike inter-sample contrastive learning, score-based intra-sample contrastive learning enforces alignment within the same video, ensuring the model learns fine-grained feature distinctions. To achieve this, we introduce two token-level prediction mechanisms early in the network: a binary score function s_t and an event category predictor c_t . We define the score function s_t as:

$$s_t = \begin{cases} 1 & \text{if } t \text{ belongs to the ground-truth event segment} \\ 0 & \text{otherwise} \end{cases} \quad (9)$$

This function is trained as a binary classifier using ground-truth labels derived from event annotations. Features within an annotated event segment are assigned a score of 1, while those outside are assigned zero via a binary cross-entropy loss.

In parallel, the model predicts an event category c_t for each feature using a cross-entropy loss over a predefined set of event classes. By jointly training s_t and c_t at the token level, the model learns both to identify the presence of an event and to classify its action, thereby refining its latent representations before final timestamp-wise decisions.

These refined token-level predictions are key to selecting meaningful samples for the intra-contrastive loss. Positive

samples are identified as features where the model accurately predicts a score of 1 (i.e., $s_t=1$) and correctly classifies the event category (c_t), ensuring alignment with the ground-truth event segments in both video and audio modalities. Hard-negative samples are features that receive a high confidence score yet are assigned an incorrect event category, challenging the model to discern subtle differences.

The process results in the identification of positive visual features I_{PV} , hard-negative visual features I_{HNV} , positive audio features I_{PA} , and hard-negative audio features I_{HNA} . These samples are then utilized in an intra-sample contrastive loss function, following a similar contrastive equation defined in Eq. (8), to enhance the model’s discriminative capabilities across modalities. The intra-contrastive loss is then formulated as:

$$\begin{aligned} \mathcal{L}_{\text{intra}} = & \mathbb{E}_{z \sim I_{PV}, z^+ \sim I_{PA}, z^- \sim I_{HNA}} \ell(z, z^+, z^-) \\ & + \mathbb{E}_{z \sim I_{PA}, z^+ \sim I_{PV}, z^- \sim I_{HNV}} \ell(z, z^+, z^-) \end{aligned} \quad (10)$$

This score-guided selection process ensures that positive samples are strongly aligned, while hard negatives provide challenging learning signals for better feature separation. Integrating hard-negative mining within intra-contrastive learning strengthens the model’s ability to differentiate between visually and aurally similar events, making it highly effective for dense event detection in untrimmed videos.

3.4. Path Aggregation Network for Multi-Scale Feature Fusion

Inspired by feature pyramid networks [8, 13, 56], we construct a multi-scale representation where lower levels focus on fine-grained temporal details while higher levels encode broader contextual information. We introduce two key components: (I) **Modality-Guided Adapters**, which enriches visual features with relevant audio cues and vice versa, ensuring better cross-modal representation. These are followed by the (II) **Adaptive Pooling Module** that dynamically adjusts feature importance across different scales, emphasizing crucial temporal cues.

In particular, the architecture processes audio features (A_{l_1}, \dots, A_{l_n}) and visual features (V_{l_1}, \dots, V_{l_n}) through top-down and bottom-up pathways to retain lower-level fine-grained details while aggregating higher-level contextual information. The modality-guided adapters employ a max-sigmoid attention mechanism to integrate audio cues into visual features,

$$V'_i = V_i \cdot \sigma \left(\max_j (V_l A_j^\top) \right)^\top, \quad (11)$$

and similarly merge visual cues into audio embeddings,

$$A'_i = A_i \cdot \sigma \left(\max_k (A_l V_k^\top) \right)^\top, \quad (12)$$

Method	0.3	0.4	0.5	0.6	0.7	Avg
MUSES [26]	68.9	64.0	56.9	46.3	31.0	-
ContextLoc [61]	68.3	63.8	54.3	41.8	26.2	50.9
A ² Net [54]	58.6	54.1	45.5	32.5	17.2	41.6
PBRNet [24]	58.5	54.6	51.3	41.8	29.5	-
AFSD [21]	67.3	62.4	55.5	43.7	31.1	52.0
TadTR [27]	62.4	57.4	49.2	37.8	26.3	46.6
Actionformer [58]	82.1	77.8	71.0	59.4	43.9	67.9
ASL [36]	83.1	79.0	71.7	59.7	45.8	66.8
TMaxer+MRVFF [11]	82.2	78.2	71.5	59.9	45.3	67.4
TriDet [38]	83.6	80.1	72.9	62.4	47.4	69.3
DEL	81.0	78.0	71.8	68.4	60.5	71.9

Table 1. **Performance comparison on THUMOS14** We report mAP across multiple tIoU thresholds and compute the average mAP. Our method outperforms previous approaches on THUMOS14 with the same feature extraction.

where σ denotes the sigmoid activation. The updated feature maps V'_i and A'_i are then combined with outputs from adjacent scales, propagating essential information throughout the pyramid. Finally, the adaptive pooling module aggregates multi-scale representations into compact tokens, \tilde{V} and \tilde{A} , and refines each modality through multi-head attention,

$$\begin{aligned} V' &= V + \text{MHA}(V, \tilde{A}, \tilde{A}) \\ A' &= A + \text{MHA}(A, \tilde{V}, \tilde{V}) \end{aligned} \quad (13)$$

where MHA denotes multi-head attention. This hierarchical design systematically fuses audio and visual cues at varying temporal scales, leading to more robust event localization and classification.

3.5. Overall Objective Function

The fused features are then passed through classification and regression heads for event category prediction and temporal boundary refinement. The final learning objective of DEL is a combination of the contrastive inter and intra losses, $\mathcal{L}_{\text{inter}}$ and $\mathcal{L}_{\text{intra}}$, and the score cross entropy loss $\mathcal{L}_{\text{score}}$. Additionally, the classification head is trained using a cross-entropy loss, \mathcal{L}_{cls} , which ensures accurate event categorization, while the regression head is optimized with a smooth L1 loss, \mathcal{L}_{reg} , to refine the temporal boundaries of each detected event:

$$\begin{aligned} \mathcal{L}_{\text{DEL}} = & \lambda_1 \mathcal{L}_{\text{inter}} + \lambda_2 \mathcal{L}_{\text{intra}} + \lambda_3 \mathcal{L}_{\text{score}} \\ & + \lambda_4 \mathcal{L}_{\text{cls}} + \lambda_5 \mathcal{L}_{\text{reg}} \end{aligned} \quad (14)$$

λ values adjust the weighting between each loss term. The values are set to balance loss terms, ensuring that no single term dominates optimization while maintaining model stability and convergence.

Method	0.5	0.75	0.95	Avg
MUSES [26]	50.0	35.0	6.6	34.0
ContextLoc [61]	56.0	35.2	3.6	34.2
VSGN [59]	52.3	35.2	8.3	34.7
A ² Net [54]	43.6	28.7	3.7	27.8
PBRNet [24]	54.0	35.0	9.0	35.0
AFSD [21]	52.4	35.3	6.5	34.4
TadTR [27]	49.1	32.6	8.5	32.3
Actionformer [58]	53.5	36.2	8.2	35.6
ASL [36]	54.1	37.4	8.0	36.2
TriDet [38]	54.7	38.0	8.4	36.8
DEL	56.9	42.5	14.7	38.0

Table 2. **Performance evaluation on ActivityNet 1.3.** We present mAP and average mAP results across various tIoU thresholds. Our approach surpasses previous methods with the same feature extraction.

4. Experiments and Results

Dataset and Metrics We conduct comprehensive evaluations on four key benchmarks: THUMOS14 [17], ActivityNet-1.3 [3], EPIC-Kitchens-100 [9], and UnAV-100 [13]. We follow the standard evaluation protocol, measuring performance using mean Average Precision (mAP) across multiple temporal Intersection over Union (tIoU) thresholds. To ensure robustness and reliability, we report averaged performance from five independent training runs to mitigate the impact of initialization.

Feature Encoder. We follow existing works, and for visual feature extraction, we used I3D [4], a two-stream inflated 3D convolutional network pretrained on Kinetics-400, for THUMOS14, ActivityNet, and UnAV-100, leveraging its effectiveness in capturing spatio-temporal dynamics. Like other works [36, 38, 58] for EPIC-Kitchens-100, where fine-grained action recognition is crucial, we employed the SlowFast network[10], pretrained on EPIC-Kitchens. Across all experiments, audio features were extracted using the VGGish model, pretrained on AudioSet [12], ensuring consistent and high-quality audio representations.

4.1. Quantitative Results

We first show the performance of our method across the range of datasets. Tab. 1 shows how on THUMOS14, our method (DEL) achieves a state-of-the-art average mAP of 71.9% (mAP@[0.3:0.1:0.7]), surpassing prior methods such as TriDet by +2.6%. Notably, DEL demonstrates superior performance at higher IoU thresholds, achieving 68.4% at 0.6 and 60.5% at 0.7, significantly outperforming existing approaches. This highlights DEL’s ability to localize actions precisely.

For ActivityNet-1.3, Tab. 2, DEL outperforms recent works with a +1.2% gain in average mAP, consistently improving across IoU thresholds. DEL performs better than

prior methods, demonstrating its effectiveness in handling large-scale datasets with diverse and long-duration activities. The model’s ability to refine event boundaries and integrate multi-scale temporal cues contributes to this improvement.

Task	Method	0.1	0.2	0.3	0.4	0.5	Avg
Verb	BMN [23]	10.8	8.8	8.4	7.1	5.6	8.4
	G-TAD [51]	12.1	11.0	9.4	8.1	6.5	9.4
	ActionFormer [58]	26.6	25.4	24.2	22.3	19.1	23.5
	ASL [36]	27.9	-	25.5	-	19.8	24.6
	ActionFormer + MRV-FF [11]	27.6	26.8	25.3	23.4	19.8	24.6
	TriDet [38]	28.6	27.4	26.1	24.2	20.8	25.4
DEL		32.2	29.9	27.8	25.1	20.8	27.1
Noun	BMN [23]	10.3	8.3	6.2	4.5	3.4	6.5
	G-TAD [51]	11.0	10.0	8.6	7.0	5.4	8.4
	ActionFormer [58]	25.2	24.1	22.7	20.5	17.0	21.9
	ASL [36]	26.0	-	23.4	-	17.7	22.6
	ActionFormer + MRV-FF [11]	26.4	25.4	23.6	21.2	17.4	22.8
	TriDet [38]	27.4	26.3	24.6	22.2	18.3	23.8
DEL		29.5	28.4	26.2	22.9	19.3	25.2

Table 3. **Performance on the EPIC-Kitchens-100 validation set** across multiple tIoU thresholds, with average mAP reported. Our method outperforms all baselines by a significant margin using the same feature extraction.

On EPIC-Kitchens-100, Tab. 3, a challenging dataset focused on fine-grained cooking activities, DEL achieves 27.1% and 25.2% average mAP for the verb and noun tasks, respectively. Compared to THUMOS14 and ActivityNet, EPIC-Kitchens presents a more complex setting with lower IoU thresholds (0.1–0.5), requiring finer temporal precision and handling of subtle action variations. DEL’s performance gain in this setting demonstrates its strength in distinguishing short, overlapping interactions through effective cross-modal alignment.

Finally, on UnAV-100, Tab. 4, a dataset featuring complex multi-event scenarios and significant audio-visual overlap, DEL achieves a state-of-the-art average mAP of 51.1%, outperforming previous methods for 3.3%. The model’s ability to capture cross-modal dependencies and adaptively fuse features across multiple temporal scales enables the robust localization of overlapping and concurrent events.

Method	0.5	0.6	0.7	0.8	0.9	Avg
VSGN [59]	24.5	20.2	15.9	11.4	6.8	24.1
TadTR [27]	30.4	27.1	23.3	19.4	14.3	29.4
ActionFormer [58]	43.5	39.4	33.4	27.3	17.9	42.2
UnAV [13]	50.6	45.8	39.8	32.4	21.1	47.8
DEL	53.4	48.1	42.6	35.6	26.9	51.1

Table 4. **Performance on the UnAV-100 test set**, showcasing our method’s significant improvement over all baselines using the same feature extraction. We report mAP and average mAP at various tIoU thresholds.

Across all benchmarks, DEL consistently improves as the IoU threshold increases, demonstrating its ability to refine temporal boundaries and focus on more confident, well-localized events. This characteristic ensures higher precision and fewer false positives, making DEL a robust choice for real-world applications requiring fine-grained audio-visual event localization.

4.2. Ablation Experiments

To explore the model’s performance in more detail, we ran an in-depth analysis on UnAV-100. This dataset was selected due to its complex audiovisual interactions, overlapping events, and untrimmed video format. Our study reveals that removing key modules leads to a significant performance drop, whereas multi-scale fusion and feature quality enhancement improve localization accuracy.

Component Ablation. Tab. 5 presents the results of remov-

AAC	SCL	PAN	0.5	0.6	0.7	0.8	0.9	Avg
×	✓	✓	51.1	45.7	41.0	34.5	25.8	49.6
✓	×	✓	51.5	44.7	38.7	33.3	25.8	49.7
✓	✓	×	51.3	45.0	39.4	33.8	25.3	49.5
✓	✓	✓	53.4	48.1	42.6	35.6	26.9	51.1

Table 5. **Component-wise ablation study**, evaluating the individual contributions of our proposed Adaptive Attention for Cross-Modal Alignment (AAC), Score-Based Contrastive Learning (SCL), and Path Aggregation Network for Multi-Scale Feature Fusion (PAN) modules.

ing key components, namely the adaptive attention mechanism, score-based contrastive learning, and path aggregation module. The analysis highlights the relative performance gains achieved by each component, demonstrating the effectiveness of DEL in improving generalizability and refining event localization.

Pyramid Levels. The path aggregation module fuses fea-

L	0.5	0.6	0.7	0.8	0.9	Avg
1	47.5	42.7	37.3	30.6	22.0	45.5
2	48.5	43.2	37.7	31.2	23.0	46.4
4	48.4	43.5	38.2	32.0	23.5	47.2
6	53.4	48.1	42.6	35.6	26.9	51.1
7	51.0	45.9	40.1	33.9	24.6	49.0

Table 6. Ablation study on the design of the feature pyramid. L shows the number of layers for both audio and video.

tures across multiple scales within our DEL framework. Tab. 6 details the results of evaluating our model on the UnAV-100 dataset using varying levels for visual and audio. Our analysis reveals that utilizing six pyramid levels for both modalities yields the best performance. These results suggest a critical balance; too few levels limit the capture of

multi-scale context, while excessive levels introduce redundant or noisy information. Tab. 6 reinforces that multi-scale audio-visual fusion and optimization of pyramid level design are critical for robust action localization performance.

Enhancing Feature Quality. To achieve precise event localization, the model must learn high-quality feature representations that capture modality-specific and cross-modal information. Enhancing feature quality ensures better differentiation between similar events and improves robustness against temporal inconsistencies, ultimately leading to more accurate and reliable predictions. Therefore, to explore the influence of the audio-visual feature extractors, we replace I3D with DINOv2 [31] for video and MERT-v1 [20] for audio. The results shown in Tab. 7 demonstrate that by integrating DINOv2 for video and MERT for audio, the performance does improve slightly, making our proposed method suitable for use with multiple feature extractor models.

Features	0.3	0.4	0.5	0.6	0.7	Avg
THUMOS14						
I3D+Vggish	81.0	78.0	71.8	68.4	60.5	71.9
DINOv2+MERT	81.5	79.1	73.1	70.8	64.6	73.3
UnAV-100						
I3D+Vggish	53.4	48.1	42.6	35.6	26.9	51.1
DINOv2+MERT	55.0	49.7	44.1	37.4	28.4	52.7

Table 7. Evaluation on THUMOS14 and UnAV-100 incorporating DINOv2 for video features and MERTv1 for audio features.

Impact of Different Input Modalities A core contribution of this work is the effective fusion of audio and visual modalities within the DEL framework, enabling robust event localization in complex, untrimmed videos. As shown in Tab. 8, DEL achieves a significantly superior average mAP of 51.1% when leveraging audio and video inputs. This represents a substantial performance increase compared to configurations using only audio (40.6%) or only video (37.9%), demonstrating the critical and complementary role of audio-visual information for accurate event localization. This performance gain is consistently observed across a comprehensive range of IoU thresholds (0.5 to 0.9), further underscoring the robustness and effectiveness of DEL’s multi-modal fusion strategy. These results validate the design choices in DEL and highlight the importance of multi-scale cross-modal perception and dependency modeling for advancing audio-visual scene understanding.

4.3. Qualitative Results.

In Fig. 4, we present qualitative results demonstrating the effectiveness of our DEL framework in comparison to unimodal baselines. For the first example, our model, leveraging audio and visual streams, accurately localizes events

Audio	Video	0.5	0.6	0.7	0.8	0.9	Avg
✓	×	41.6	36.3	32.7	27.8	21.6	40.6
×	✓	38.3	33.4	28.9	25.2	19.2	37.9
✓	✓	53.4	48.1	42.6	35.6	26.9	51.1

Table 8. DEL performance with various modality combinations. Fusing audio and video yields the best results, emphasizing the importance of multi-modal input.

such as wind noise, cars passing by, driving a motorcycle, and skidding, even in scenarios with overlapping or short-duration occurrences. In contrast, the audio-only model struggles with visually-driven events like skidding, while the vision-only model fails to detect sound-based events like wind noise. Moreover, relying solely on audio leads to incorrect predictions, such as misclassifying the scene as engine knocking due to the absence of visual context. Similarly, the vision-only model, lacking critical audio cues, misinterprets the scene as auto racing from start to finish, based purely on visual perception. This shows the impact of audio in disambiguating visually similar activities. Distinguishing between "man speaking" and another potential sound source in the third scenario is only possible with audio input, as visual information alone is insufficient.

Similarly, in the last example, the scene is crowded, making it challenging to infer "people cheering" using only visual cues. The vision-only model struggles to recognize this category, while the audio modality provides crucial information for its correct identification. Additionally, detecting "people slapping" relies primarily on visual cues. These results highlight how integrating audio and visual streams leads to more accurate and robust event localization, particularly in complex multimodal scenarios.

These results highlight the complementary nature of audio and visual modalities for precise dense event localization, particularly in complex, real-world scenarios where events are often overlapping and context-dependent.

5. Conclusion

This paper introduced DEL, a dense audio-visual event localization framework for untrimmed videos. DEL effectively tackles the challenges of overlapping events and complex temporal dependencies by dynamically aligning audio and visual representations with an adaptive attention mechanism and a novel contrastive learning strategy. The vision-audio path aggregation network further strengthens cross-modal interactions, enabling deeper audio-visual feature integration at multiple temporal resolutions. With state-of-the-art performance on UnAV-100, THUMOS14, ActivityNet 1.3, and EPIC-Kitchens-100, DEL redefines fine-grained semantic action localization, paving the way for more sophisticated audio-visual scene understanding. DEL advances the field by bridging the gap between

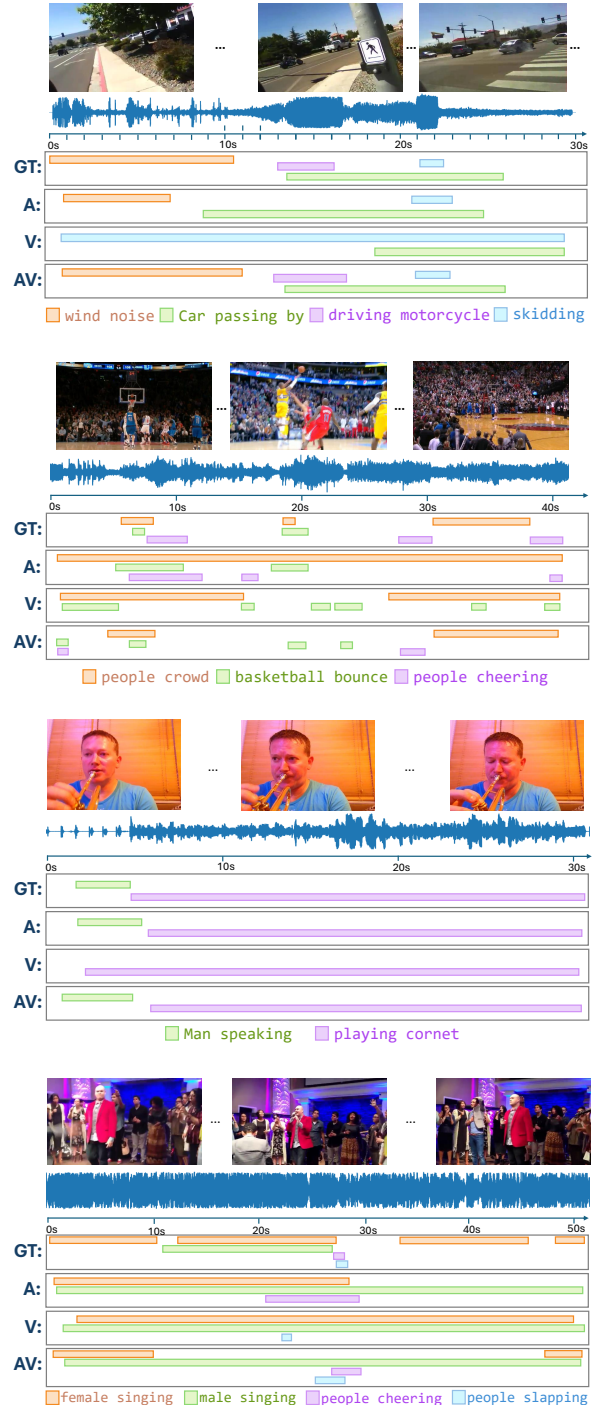


Figure 4. Qualitative results of our DEL framework for audio-visual event localization. We present ground-truth (GT) and event categories alongside predictions from audio-only (A), vision-only (V), and audio-visual (AV) models. The AV model (DEL) achieves more accurate event localization by effectively leveraging both modalities, while the unimodal models struggle with events that rely on cross-modal cues.

existing methodologies and real-world video analysis. It sparks new possibilities for future research in uncovering even richer insights from complex video content.

References

- [1] Juan León Alcázar, Fabian Caba, Ali K Thabet, and Bernard Ghanem. Maas: Multi-modal assignment for active speaker detection. In *Proceedings of the IEEE/CVF International Conference on Computer Vision*, pages 265–274, 2021. 2
- [2] Anurag Bagchi, Jazib Mahmood, Dolton Fernandes, and Ravi Kiran Sarvadevabhatla. Hear me out: Fusional approaches for audio augmented temporal action localization. *arXiv preprint arXiv:2106.14118*, 2021. 2
- [3] Fabian Caba Heilbron, Victor Escorcia, Bernard Ghanem, and Juan Carlos Niebles. Activitynet: A large-scale video benchmark for human activity understanding. In *Proceedings of the IEEE conference on computer vision and pattern recognition*, pages 961–970, 2015. 1, 2, 6
- [4] Joao Carreira and Andrew Zisserman. Quo vadis, action recognition? a new model and the kinetics dataset. In *proceedings of the IEEE Conference on Computer Vision and Pattern Recognition*, pages 6299–6308, 2017. 6, 1
- [5] Shuning Chang, Pichao Wang, Fan Wang, Hao Li, and Zheng Shou. Augmented transformer with adaptive graph for temporal action proposal generation. In *Proceedings of the 3rd International Workshop on Human-Centric Multimedia Analysis*, pages 41–50, 2022. 2
- [6] Yu-Wei Chao, Sudheendra Vijayanarasimhan, Bryan Seybold, David A Ross, Jia Deng, and Rahul Sukthankar. Rethinking the faster r-cnn architecture for temporal action localization. In *Proceedings of the IEEE conference on computer vision and pattern recognition*, pages 1130–1139, 2018. 2
- [7] Feng Cheng and Gedas Bertasius. Tallformer: Temporal action localization with a long-memory transformer. In *European Conference on Computer Vision*, pages 503–521. Springer, 2022. 2
- [8] Tianheng Cheng, Lin Song, Yixiao Ge, Wenyu Liu, Xinggang Wang, and Ying Shan. Yolo-world: Real-time open-vocabulary object detection. In *Proceedings of the IEEE/CVF Conference on Computer Vision and Pattern Recognition*, pages 16901–16911, 2024. 2, 5
- [9] Dima Damen, Hazel Doughty, Giovanni Maria Farinella, Antonino Furnari, Evangelos Kazakos, Jian Ma, Davide Moltisanti, Jonathan Munro, Toby Perrett, Will Price, et al. Rescaling egocentric vision: Collection, pipeline and challenges for epic-kitchens-100. *International Journal of Computer Vision*, pages 1–23, 2022. 1, 2, 6
- [10] Christoph Feichtenhofer, Haoqi Fan, Jitendra Malik, and Kaiming He. Slowfast networks for video recognition. In *Proceedings of the IEEE/CVF international conference on computer vision*, pages 6202–6211, 2019. 6, 1
- [11] Edward Fish, Jon Weinren, and Andrew Gilbert. Multi-resolution audio-visual feature fusion for temporal action localization. *arXiv preprint arXiv:2310.03456*, 2023. 5, 6, 3
- [12] Jort F Gemmeke, Daniel PW Ellis, Dylan Freedman, Aren Jansen, Wade Lawrence, R Channing Moore, Manoj Plakal, and Marvin Ritter. Audio set: An ontology and human-labeled dataset for audio events. In *2017 IEEE international conference on acoustics, speech and signal processing (ICASSP)*, pages 776–780. IEEE, 2017. 1, 6
- [13] Tiantian Geng, Teng Wang, Jinming Duan, Runmin Cong, and Feng Zheng. Dense-localizing audio-visual events in untrimmed videos: A large-scale benchmark and baseline. In *Proceedings of the IEEE/CVF Conference on Computer Vision and Pattern Recognition*, pages 22942–22951, 2023. 1, 2, 5, 6, 3
- [14] Kaiming He, Haoqi Fan, Yuxin Wu, Saining Xie, and Ross Girshick. Momentum contrast for unsupervised visual representation learning. In *Proceedings of the IEEE/CVF conference on computer vision and pattern recognition*, pages 9729–9738, 2020. 4
- [15] Shawn Hershey, Sourish Chaudhuri, Daniel PW Ellis, Jort F Gemmeke, Aren Jansen, R Channing Moore, Manoj Plakal, Devin Platt, Rif A Saurous, Bryan Seybold, et al. Cnn architectures for large-scale audio classification. In *2017 IEEE international conference on acoustics, speech and signal processing (icassp)*, pages 131–135. IEEE, 2017. 2
- [16] Xixi Hu, Ziyang Chen, and Andrew Owens. Mix and localize: Localizing sound sources in mixtures. In *Proceedings of the IEEE/CVF Conference on Computer Vision and Pattern Recognition*, pages 10483–10492, 2022. 2
- [17] Haroon Idrees, Amir R Zamir, Yu-Gang Jiang, Alex Gorban, Ivan Laptev, Rahul Sukthankar, and Mubarak Shah. The thumos challenge on action recognition for videos “in the wild”. *Computer Vision and Image Understanding*, 155:1–23, 2017. 1, 2, 6
- [18] Licheng Jiao, Yuhan Wang, Xu Liu, Lingling Li, Fang Liu, Wenping Ma, Yuwei Guo, Puhua Chen, Shuyuan Yang, and Biao Hou. Causal inference meets deep learning: A comprehensive survey. *Research*, 7:0467, 2024. 1
- [19] Evangelos Kazakos, Arsha Nagrani, Andrew Zisserman, and Dima Damen. Epic-fusion: Audio-visual temporal binding for egocentric action recognition. In *Proceedings of the IEEE/CVF international conference on computer vision*, pages 5492–5501, 2019. 2
- [20] Yizhi Li, Ruibin Yuan, Ge Zhang, Yinghao Ma, Xingran Chen, Hanzhi Yin, Chenghao Xiao, Chenghua Lin, Anton Ragni, Emmanouil Benetos, et al. Mert: Acoustic music understanding model with large-scale self-supervised training. *arXiv preprint arXiv:2306.00107*, 2023. 7
- [21] Chuming Lin, Chengming Xu, Donghao Luo, Yabiao Wang, Ying Tai, Chengjie Wang, Jilin Li, Feiyue Huang, and Yanwei Fu. Learning salient boundary feature for anchor-free temporal action localization. In *Proceedings of the IEEE/CVF conference on computer vision and pattern recognition*, pages 3320–3329, 2021. 2, 5, 6, 1
- [22] Tianwei Lin, Xu Zhao, Haisheng Su, Chongjing Wang, and Ming Yang. Bsn: Boundary sensitive network for temporal action proposal generation. In *Proceedings of the European conference on computer vision (ECCV)*, pages 3–19, 2018. 2, 1

- [23] Tianwei Lin, Xiao Liu, Xin Li, Errui Ding, and Shilei Wen. Bmn: Boundary-matching network for temporal action proposal generation. In *Proceedings of the IEEE/CVF international conference on computer vision*, pages 3889–3898, 2019. 2, 6, 1, 3
- [24] Qinying Liu and Zilei Wang. Progressive boundary refinement network for temporal action detection. In *Proceedings of the AAAI conference on artificial intelligence*, pages 11612–11619, 2020. 5, 6
- [25] Shuo Liu, Weize Quan, Chaoqun Wang, Yuan Liu, Bin Liu, and Dong-Ming Yan. Dense modality interaction network for audio-visual event localization. *IEEE Transactions on Multimedia*, 25:2734–2748, 2022. 2
- [26] Xiaolong Liu, Yao Hu, Song Bai, Fei Ding, Xiang Bai, and Philip HS Torr. Multi-shot temporal event localization: a benchmark. In *Proceedings of the IEEE/CVF Conference on Computer Vision and Pattern Recognition*, pages 12596–12606, 2021. 5, 6
- [27] Xiaolong Liu, Qimeng Wang, Yao Hu, Xu Tang, Shiwei Zhang, Song Bai, and Xiang Bai. End-to-end temporal action detection with transformer. *IEEE Transactions on Image Processing*, 31:5427–5441, 2022. 5, 6
- [28] Fuchen Long, Ting Yao, Zhaofan Qiu, Xinmei Tian, Jiebo Luo, and Tao Mei. Gaussian temporal awareness networks for action localization. In *Proceedings of the IEEE/CVF conference on computer vision and pattern recognition*, pages 344–353, 2019. 2
- [29] Sauradip Nag, Xiatian Zhu, Yi-Zhe Song, and Tao Xiang. Proposal-free temporal action detection via global segmentation mask learning. In *European Conference on Computer Vision*, pages 645–662. Springer, 2022. 2
- [30] Arsha Nagrani, Shan Yang, Anurag Arnab, Aren Jansen, Cordelia Schmid, and Chen Sun. Attention bottlenecks for multimodal fusion. *Advances in neural information processing systems*, 34:14200–14213, 2021. 1
- [31] Maxime Oquab, Timothée Darcet, Théo Moutakanni, Huy Vo, Marc Szafraniec, Vasil Khalidov, Pierre Fernandez, Daniel Haziza, Francisco Massa, Alaaeldin El-Nouby, et al. Dinov2: Learning robust visual features without supervision. *arXiv preprint arXiv:2304.07193*, 2023. 7
- [32] Andrew Owens and Alexei A Efros. Audio-visual scene analysis with self-supervised multisensory features. In *Proceedings of the European conference on computer vision (ECCV)*, pages 631–648, 2018. 1
- [33] Arjun Prashanth, SL Jayalakshmi, and R Vedhapriyavadhana. A review of deep learning techniques in audio event recognition (aer) applications. *Multimedia Tools and Applications*, 83(3):8129–8143, 2024. 1
- [34] Merey Ramazanova, Victor Escorcía, Fabian Caba, Chen Zhao, and Bernard Ghanem. Owl (observe, watch, listen): Audiovisual temporal context for localizing actions in ego-centric videos. In *Proceedings of the IEEE/CVF Conference on Computer Vision and Pattern Recognition*, pages 4879–4889, 2023. 2
- [35] Joseph Redmon, Santosh Divvala, Ross Girshick, and Ali Farhadi. You only look once: Unified, real-time object detection. In *Proceedings of the IEEE conference on computer vision and pattern recognition*, pages 779–788, 2016. 2
- [36] Jiayi Shao, Xiaohan Wang, Ruijie Quan, Junjun Zheng, Jiang Yang, and Yi Yang. Action sensitivity learning for temporal action localization. In *Proceedings of the IEEE/CVF International Conference on Computer Vision*, pages 13457–13469, 2023. 5, 6
- [37] Dingfeng Shi, Qiong Cao, Yujie Zhong, Shan An, Jian Cheng, Haogang Zhu, and Dacheng Tao. Temporal action localization with enhanced instant discriminability. *arXiv preprint arXiv:2309.05590*, 2023. 2
- [38] Dingfeng Shi, Yujie Zhong, Qiong Cao, Lin Ma, Jia Li, and Dacheng Tao. Tridet: Temporal action detection with relative boundary modeling. In *Proceedings of the IEEE/CVF Conference on Computer Vision and Pattern Recognition*, pages 18857–18866, 2023. 5, 6
- [39] Jing Tan, Jiaqi Tang, Limin Wang, and Gangshan Wu. Relaxed transformer decoders for direct action proposal generation. In *Proceedings of the IEEE/CVF international conference on computer vision*, pages 13526–13535, 2021. 2
- [40] Yapeng Tian, Jing Shi, Bochen Li, Zhiyao Duan, and Chenliang Xu. Audio-visual event localization in unconstrained videos. In *Proceedings of the European conference on computer vision (ECCV)*, pages 247–263, 2018. 1, 2
- [41] Elahe Vahdani and Yingli Tian. Deep learning-based action detection in untrimmed videos: A survey. *IEEE Transactions on Pattern Analysis and Machine Intelligence*, 45(4):4302–4320, 2022. 1
- [42] Satvik Venkatesh, David Moffat, and Eduardo Reck Miranda. You only hear once: a yolo-like algorithm for audio segmentation and sound event detection. *Applied Sciences*, 12(7):3293, 2022. 1
- [43] Lining Wang, Haosen Yang, Wenhao Wu, Hongxun Yao, and Hujie Huang. Temporal action proposal generation with transformers. *arXiv preprint arXiv:2105.12043*, 2021. 2
- [44] Qiang Wang, Yanhao Zhang, Yun Zheng, and Pan Pan. Rcl: Recurrent continuous localization for temporal action detection. In *Proceedings of the IEEE/CVF conference on computer vision and pattern recognition*, pages 13566–13575, 2022. 2
- [45] Yi Wang, Kunchang Li, Xinhao Li, Jiashuo Yu, Yanan He, Guo Chen, Baoqi Pei, Rongkun Zheng, Zun Wang, Yansong Shi, et al. Internvideo2: Scaling foundation models for multimodal video understanding. In *European Conference on Computer Vision*, pages 396–416. Springer, 2024. 2
- [46] Yuetian Weng, Zizheng Pan, Mingfei Han, Xiaojun Chang, and Bohan Zhuang. An efficient spatio-temporal pyramid transformer for action detection. In *European Conference on Computer Vision*, pages 358–375. Springer, 2022. 2
- [47] Yu Wu, Linchao Zhu, Yan Yan, and Yi Yang. Dual attention matching for audio-visual event localization. In *Proceedings of the IEEE/CVF international conference on computer vision*, pages 6292–6300, 2019. 2
- [48] Kun Xia, Le Wang, Sanping Zhou, Gang Hua, and Wei Tang. Dual relation network for temporal action localization. *Pattern Recognition*, 129:108725, 2022. 2
- [49] Kun Xia, Le Wang, Sanping Zhou, Nanning Zheng, and Wei Tang. Learning to refactor action and co-occurrence features for temporal action localization. In *Proceedings of*

- the IEEE/CVF conference on computer vision and pattern recognition*, pages 13884–13893, 2022. [2](#)
- [50] Fanyi Xiao, Yong Jae Lee, Kristen Grauman, Jitendra Malik, and Christoph Feichtenhofer. Audiovisual slowfast networks for video recognition. *arXiv preprint arXiv:2001.08740*, 2020. [2](#)
- [51] Mengmeng Xu, Chen Zhao, David S Rojas, Ali Thabet, and Bernard Ghanem. G-tad: Sub-graph localization for temporal action detection. In *Proceedings of the IEEE/CVF conference on computer vision and pattern recognition*, pages 10156–10165, 2020. [2](#), [6](#)
- [52] Cheng Xue, Xionghu Zhong, Minjie Cai, Hao Chen, and Wenwu Wang. Audio-visual event localization by learning spatial and semantic co-attention. *IEEE Transactions on Multimedia*, 25:418–429, 2021. [2](#)
- [53] Ceyuan Yang, Yinghao Xu, Jianping Shi, Bo Dai, and Bolei Zhou. Temporal pyramid network for action recognition. In *Proceedings of the IEEE/CVF conference on computer vision and pattern recognition*, pages 591–600, 2020. [2](#)
- [54] Le Yang, Houwen Peng, Dingwen Zhang, Jianlong Fu, and Junwei Han. Revisiting anchor mechanisms for temporal action localization. *IEEE Transactions on Image Processing*, 29:8535–8548, 2020. [2](#), [5](#), [6](#)
- [55] Jiashuo Yu, Ying Cheng, and Rui Feng. Mpn: Multimodal parallel network for audio-visual event localization. In *2021 IEEE International Conference on Multimedia and Expo (ICME)*, pages 1–6. IEEE, 2021. [2](#)
- [56] Jiashuo Yu, Ying Cheng, Rui-Wei Zhao, Rui Feng, and Yuejie Zhang. Mm-pyramid: Multimodal pyramid attentional network for audio-visual event localization and video parsing. In *Proceedings of the 30th ACM international conference on multimedia*, pages 6241–6249, 2022. [5](#)
- [57] Runhao Zeng, Wenbing Huang, Mingkui Tan, Yu Rong, Peilin Zhao, Junzhou Huang, and Chuang Gan. Graph convolutional networks for temporal action localization. In *Proceedings of the IEEE/CVF international conference on computer vision*, pages 7094–7103, 2019. [2](#)
- [58] Chen-Lin Zhang, Jianxin Wu, and Yin Li. Actionformer: Localizing moments of actions with transformers. In *European Conference on Computer Vision*, pages 492–510. Springer, 2022. [2](#), [5](#), [6](#), [1](#), [3](#)
- [59] Chen Zhao, Ali K Thabet, and Bernard Ghanem. Video self-stitching graph network for temporal action localization. In *Proceedings of the IEEE/CVF International Conference on Computer Vision*, pages 13658–13667, 2021. [2](#), [6](#)
- [60] Peisen Zhao, Lingxi Xie, Chen Ju, Ya Zhang, Yanfeng Wang, and Qi Tian. Bottom-up temporal action localization with mutual regularization. In *Computer Vision—ECCV 2020: 16th European Conference, Glasgow, UK, August 23–28, 2020, Proceedings, Part VIII 16*, pages 539–555. Springer, 2020. [1](#)
- [61] Zixin Zhu, Wei Tang, Le Wang, Nanning Zheng, and Gang Hua. Enriching local and global contexts for temporal action localization. In *Proceedings of the IEEE/CVF international conference on computer vision*, pages 13516–13525, 2021. [5](#), [6](#)

DEL: Dense Event Localization for Multi-modal Audio-Visual Understanding

Supplementary Material

6. Experimental Details

We present the implementation details, including the network architecture, training process, and inference strategy. Our code provides further information.

6.1. Evaluation Metric: Mean Average Precision (mAP)

In temporal action localization, mean Average Precision (mAP) is the most commonly used evaluation metric, with t-IoU = 0.5 as a standard comparison reference point.

Precision (P) measures the proportion of correctly detected action instances within a single class for a given video. Specifically, for class C, precision is defined as:

$$P = \frac{TP}{TP + FP} = \frac{\text{Number of correctly predicted proposals}}{\text{Total number of predicted proposals}} \quad (15)$$

Since the test set contains multiple videos, Average Precision (AP) represents the mean precision for a specific class C across all test videos. Further, as the test set spans multiple action classes, the mean Average Precision (mAP) is computed as the mean of AP values across all classes:

$$mAP = \frac{\sum AP}{\text{Total number of classes}} \quad (16)$$

In summary, under a given t-IoU threshold, Precision (P) quantifies the accuracy of detected action instances within a specific class in a single video, AP reflects the averaged precision across all classes in a video, and mAP generalizes this across all test videos and classes. Following standard evaluation protocols, most studies report mAP at multiple t-IoU thresholds to assess model performance comprehensively.

6.2. Datasets

Our experimental setup differs across datasets due to variations in video resolution, frame rates, and feature types. Below, we provide specific details for THUMOS14, ActivityNet-1.3, EPIC-Kitchens-100, and UnAV100. THUMOS14 consists of 413 untrimmed videos from 20 action classes, utilizing 200 validation videos for training and 213 test videos for evaluation. ActivityNet v1.3, a large-scale dataset with over 20,000 videos, spans 200 action categories, containing 10,024 training videos and 4,926 validation videos. ActivityNet v1.2, a subset of v1.3, includes 100 action categories with 4,819 training and 2,383 validation videos. EPIC-Kitchens-100 contains 100 hours of cooking activities in kitchens. It has two tasks: noun localization (300 classes) and verb localization (97). While UnAV-

100 contains 30,059 audiovisual events across 100 categories within 10,790 untrimmed videos, totaling over 126 video hours. Approximately 60% of videos contain multiple audio-visual events, averaging 2.8 events per video, and around 25% include concurrent events.

- **THUMOS14:** For feature extraction on THUMOS14, we utilized a two-stream I3D model [4] pretrained on Kinetics, aligning with [58, 60]. Each input clip consisted of 16 consecutive frames, processed using a sliding window with a stride of 4. We extracted 1024-D features from the layer preceding the final fully connected layer and combined the two-stream outputs into a 2048-D representation as input to our model. Performance was assessed using mAP across tIoU thresholds in the range [0.3:0.1:0.7]. The model was trained for 50 epochs, starting with a 5-epoch linear warmup. The learning rate was initialized at $5e-4$. To improve generalization, a cosine decay schedule with a weight decay of $1e-4$ was applied.
- **ActivityNet-1.3** We utilized a two-stream I3D model [4] for feature extraction, setting the sliding window stride to 16. Following previous studies [22, 23, 58], features were downsampled to fixed lengths of 160 using linear interpolation for I3D features. Performance was measured using $mAP@[0.5:0.05:0.95]$, along with the average mAP. The model was trained for 15 epochs with a 5-epoch linear warmup, using a learning rate of $5e-4$, and a weight decay of $1e-4$. For ActivityNet, we adopted a proposal generation strategy that groups all actions within a single category, followed by external classification scoring for recognition, a technique proven effective in prior single-stage temporal action localization approaches [21].
- **EPIC-Kitchens-100** We extracted features using a Slow-Fast network [10], which was pretrained on EPIC-Kitchens-100 and provided by [9]. The model processed 32-frame video segments with a stride of 16, generating 2304-dimensional feature embeddings. Training was conducted on the designated training split, while evaluation was performed on the validation set. For evaluation, we followed the $mAP@[0.1:0.1:0.5]$ metric and reported the average mAP, maintaining consistency with [9]. The model was trained for 30 epochs, using an initial learning rate of $5e-4$ and a weight decay of $1e-4$, ensuring stable convergence.
- **UnAV100** For processing UnAV-100, we extract visual and audio features while ensuring proper temporal alignment. Video frames are sampled at 25 fps, and for each segment, we use a two-stream I3D [4] network to process 24 consecutive RGB and optical flow frames. A stride of 8 is applied during feature extraction, and the out-

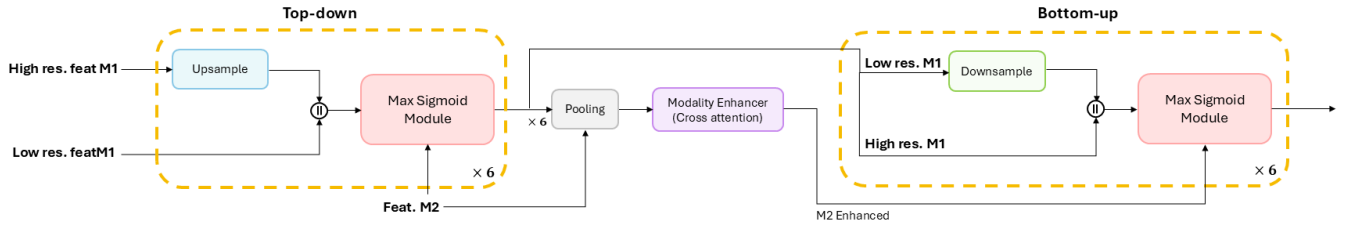


Figure 5. Illustration of the Path Aggregation Network for multi-scale feature fusion. The network employs a top-down and bottom-up pathway to fuse feature maps from different temporal scales, which helps capture fine-grained details and high-level semantics. A modality enhancer module refines cross-modal feature representations by applying cross-attention, ensuring robust integration of audio-visual data for accurate event localization. M1 indicates one modality (e.g., visual), and M2 represents the other (e.g., audio). \parallel represents the concatenation operation. The details of the max sigmoid module are shown Fig. 6.

puts from both streams are concatenated to form a 2048-dimensional visual representation. Simultaneously, VG-Gish [15] extracts audio embeddings from 0.96-second segments with a stride of 0.32 seconds, ensuring synchronization with the visual features. Since video lengths vary, we standardize inputs by cropping or padding sequences to a fixed length of $T = 224$.

For training, we adopt the Adam optimizer and run the model for 40 epochs, incorporating a 5-epoch linear warmup at the start. The initial learning rate is set to $1e-3$ and follows a cosine decay schedule for smoother optimization. We apply weight decay of $1e-4$ to regularize training. Given that UnAV-100 focuses on temporal event localization in untrimmed videos, we evaluate model performance using mean Average Precision (mAP). Specifically, we compute mAP at tIoU thresholds from 0.5 to 0.9 (step size 0.1) and report the average mAP over the range 0.1 to 0.9, ensuring a robust assessment of localization accuracy.

7. Path Aggregation Network for Multi-Scale Feature Fusion

We propose a path aggregation network to ensure information is aggregated across multiple temporal resolutions, preserving short-term event cues and long-term contextual dependencies. This approach ensures greater feature consistency across different temporal resolutions, ultimately improving the regression of an event’s location.

As illustrated in Fig. 5, we employ top-down and bottom-up pathways to construct a feature pyramid. This design integrates multi-scale visual features (V_{l_1} to V_{l_n}) and multi-scale audio features (A_{l_1} to A_{l_n}) into a series of feature pyramids (P_1 through P_n). Lower levels capture fine-grained temporal details, while higher levels encode abstract, long-term dependencies. To enhance the interplay between visual and audio features, our network introduces two key components: (I) a **Audio & Visual-guided**

Adapters and (II) an **Adaptive Pooling Module**. The audio-guided adapter enriches visual features with acoustic context, while the visual-guided adapter enhances audio representations with visual semantics. These are followed by the adaptive pooling module that refines cross-modal integration by dynamically adjusting feature importance across different scales, ensuring optimal weighting of short- and long-duration event cues.

7.1. Modality-guided Adapters:

These adapted modality-guided adapters are strategically positioned after the top-down or bottom-up fusion processes to leverage information from both modalities for mutual enrichment. For the audio-guided adapter features, let $A_l \in \mathbb{R}^{T_A \times d}$ represent the audio embeddings and $V_l \in \mathbb{R}^{T_V \times d}$ (where $l \in \{1, 2, 3, 4, 5, 6\}$) denote the visual features in different scales. We then apply max-sigmoid attention to integrate the audio features into the visual features:

$$V'_l = V_l \cdot \delta \left(\max_{j \in \{1..C_A\}} (V_l A_j^T) \right)^T \quad (17)$$

where the δ represents the sigmoid activation function.

Similarly, for the visual-guided adapter, we apply max-sigmoid attention to integrate visual features into audio features:

$$A'_l = A_l \cdot \delta \left(\max_{k \in \{1..C_V\}} (A_l V_k^T) \right)^T \quad (18)$$

In both equations, V'_l and A'_l represent the updated feature maps for video and audio, respectively, which are then concatenated with their corresponding cross-stage features to produce the final outputs. Note that C_A and C_V represent the number of audio and video embedding channels, respectively.

7.2. Adaptive Pooling Module (APM)

To further enhance the video features with audio information, the APM aggregates multi-scale audio features into N

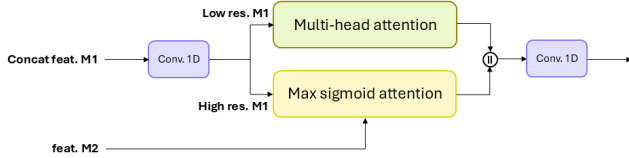


Figure 6. Detailed diagram of the max sigmoid module. This module is a key component of our path aggregation network, facilitating adaptive feature fusion between modalities. It takes high- and low-resolution feature maps from modality M1 and combines them with features from modality M2, using a max sigmoid function to dynamically select the most relevant features for enhanced representation learning.

temporal segments, resulting in audio tokens $\tilde{A} \in \mathbb{R}^{N \times d}$. We aggregate multi-scale audio features into N temporal segments to establish a shared temporal resolution between audio and video modalities. Since the extracted audio and video features may have different temporal resolutions due to variations in sampling rates and processing pipelines, directly aligning them can be challenging. By fixing both modalities to N segments, we enforce a structured representation where each token captures a comparable temporal extent across both modalities, ensuring better temporal synchronization between audio and video. This normalization reduces modality mismatches and allows multi-head attention to operate more effectively by aligning the most relevant audio cues with corresponding video segments. Additionally, this strategy helps manage computational efficiency by reducing the number of tokens processed while maintaining rich cross-modal interactions. These tokens are then used to update the video embeddings V through multi-head attention:

$$V' = V + \text{MultiHead-Attention}(V, \tilde{A}, \tilde{A}) \quad (19)$$

Conversely, for audio enhancement, the APM aggregates multi-scale video features into N spatial regions, producing video tokens $\tilde{V} \in \mathbb{R}^{N \times d}$. These tokens update the audio embeddings A :

$$A' = A + \text{MultiHead-Attention}(A, \tilde{V}, \tilde{V}) \quad (20)$$

This approach allows for efficient integration of audio context into video representations and vice versa. The resulting updated embeddings, V' and A' , offer richer cross-modal representations that improve the overall performance of our audio-visual fusion network.

7.3. Limitations and Future Works

While DEL demonstrates strong performance in dense audio-visual event localization, certain limitations remain. First, like many previous approaches [11, 13, 23, 58], the

model depends on pre-extracted features. Exploring end-to-end trainable feature extractors could further enhance performance. Second, DEL primarily focuses on audio-visual fusion but does not explicitly incorporate language-based cues, which could provide richer contextual understanding, especially for complex multi-event scenarios. Finally, expanding the framework to handle unseen categories through few-shot or self-supervised learning techniques could improve its robustness and generalization in open-world settings.